Published in final edited form as:

*Clin Cancer Res*. 2019 March 01; 25(5): 1588–1600. doi:10.1158/1078-0432.CCR-17-2730.

# Ablation of cancer stem cells by therapeutic inhibition of the MDM2-p53 interaction in mucoepidermoid carcinoma

**April Andrews**[1], **Kristy Warner**[1], **Christie Rodriguez-Ramirez**[1], **Alexander T. Pearson**[2], **Felipe Nör**[1], **Zhaocheng Zhang**[1], **Samuel Kerk**[1], **Aditi Kulkarni**[3], **Joseph I. Helman**[4], **J. Chad Brenner**[3,5,6], **Max S. Wicha**[6,7], **Shaomeng Wang**[6,8], and **Jacques E. Nör**[1,3,6,9]

[1]Department of Cariology, Restorative Sciences, Endodontics, University of Michigan School of Dentistry, Ann Arbor, MI

[2]Department of Medicine, University of Chicago, Chicago, IL

[3]Department of Otolaryngology, University of Michigan School of Medicine, Ann Arbor, MI

[4]Department of Oral and Maxillofacial Surgery, University of Michigan School of Medicine, Ann Arbor, MI

[5]Department of Pharmacology, University of Michigan, Ann Arbor, MI

[6]Rogel Cancer Center, University of Michigan School of Medicine, Ann Arbor, MI

[7]Department of Internal Medicine, University of Michigan School of Medicine, Ann Arbor, MI

[8]Department of Medicinal Chemistry, University of Michigan, Ann Arbor, MI

[9]Department of Biomedical Engineering, University of Michigan College of Engineering, Ann Arbor, MI

## Abstract

**Purpose:** Unique cells characterized by multipotency, self-renewal and high tumorigenic potential have been recently discovered in mucoepidermoid carcinomas (MEC). These cells are defined by high aldehyde dehydrogenase activity and high CD44 expression ($ALDH^{high}CD44^{high}$) and function as cancer stem cells. It has been recently shown that p53 regulates cell differentiation, suggesting that induction of p53 by therapeutic blockade of the MDM2-p53 interaction may constitute a novel strategy to ablate cancer stem cells. Here, we evaluated the effect of a small molecule inhibitor of MDM2-p53 interaction (MI-773) on the fraction of cancer stem cells in mucoepidermoid carcinoma.

**Experimental design:** Human mucoepidermoid carcinoma cells (UM-HMC-1,−3A,−3B) were used to assess the effect of MI-773 on cell survival, cell cycle, fraction of cancer stem cells and expression of p53, p21, MDM2, and Bmi-1 (key regulator of self-renewal). Mice bearing

**Corresponding Author**, Jacques E. Nör DDS, PhD, Professor of Dentistry, Biomedical Engineering, Otolaryngology, University of Michigan, 1011 N. University Rm. 2361, Ann Arbor, MI, 48109-1078, United States, Telephone: (734) 936-9300, jenor@umich.edu.

Conflict of Interest

Shaomeng Wang is the inventor of MI-773, which is being developed by Ascenta and Sanofi and received royalties from the University of Michigan. Dr. Shaomeng Wang also owns stock in Ascenta and has received research funding from Ascenta and Sanofi.

xenograft tumors generated with these MEC cells were treated with MI-773 to determine the effect of MDM2-p53 inhibition on cancer stem cells *in vivo.*

**Results:** MDM2 is highly expressed in human MEC tissues. MI-773 induced expression of p53 and its downstream targets p21 and MDM2, caused $G_1$ cell cycle arrest, and induced MEC tumor cell apoptosis *in vitro*. Importantly, a marked decrease in expression of Bmi-1 and in the fraction of $ALDH^{high}CD44^{high}$ (cancer stem cells) was caused by MI-773 *in vitro* and in mice harboring MEC xenografts.

**Conclusion:** Collectively, these data demonstrate that MI-773 reduces the fraction of cancer stem cells, suggesting that patients with mucoepidermoid carcinoma might benefit from therapeutic inhibition of the MDM2-p53 interaction.

### Keywords

Tumor-initiating cells; Differentiation; Apoptosis; Mucoepidermoid carcinoma; Salivary gland cancer

## Introduction

Salivary gland mucoepidermoid carcinomas (MEC) are the most common salivary malignancy, accounting for 30–35% of all malignant salivary gland tumors (1–8). Patients diagnosed with mucoepidermoid carcinomas are treated using surgical resection and radiation therapies (9). While surgery is often sufficient for patients with low to intermediate grade tumors, patients with high-grade tumors often display recurrent disease (10). As mucoepidermoid carcinomas are resistant to chemotherapy, treatment of patients with local-regional recurrence involves radiotherapy, but the long-term prognosis of these patients is modest (10,11). Improved understanding of the pathobiology of MEC is essential for the identification of more effective therapies that prevent local-regional recurrence and enhance the survival of MEC patients.

A subpopulation of cells, termed cancer stem cells (CSC), is uniquely tumorigenic and capable of multipotency and self-renewal. Cancer stem cells are essential for both initiating and maintaining the growth of many cancer types (12). Importantly, cancer stem cells are resistance to conventional chemotherapies and radiation treatments due to their slow proliferation, the presence of transporter proteins that facilitate cell detoxification, as well as micro-environmental influences that enhance their survival (13–15). It has been postulated that survival of cancer stem cells after treatment allows for tumor regrowth and recurrence (16–17). We have recently identified functionally the existence of cancer stem cells in salivary gland mucoepidermoid carcinomas (18). MEC cells sorted for $ALDH^{high}CD44^{high}$ exhibit self-renewal and multipotency, and are highly tumorigenic when compared to control cells. Selective targeting and ablation of $ALDH^{high}CD44^{high}$ cells might be a novel approach to prevent local-regional recurrences in patients with mucoepidermoid carcinoma.

p53 functions as a transcription factor that plays an essential role in many cellular functions, including regulation of cell cycle and senescence, as well as induction of apoptosis upon the genomic damage (19–21). The function of p53 in adult and embryonic stem cell differentiation has been described more recently. In normal differentiated cells, deletion or

repression of p53 function leads to greater efficiency in dedifferentiating into induced pluripotent stem cells (22–26). In the context of cancer, research has shown that loss of p53 also led to the expansion of malignant reprogrammed progenitor cells in liver cancer (27). Mouse double minute (MDM) 2 regulates p53 by binding to it and signaling its degradation by the proteasome (28). Indeed, MDM2 is an oncogene that is overexpressed in many cancers, including salivary gland tumors (29).

Over the last few years, small molecule inhibitors of the MDM2 binding to p53 have been developed. One small molecule in particular, MI-773, has been shown to have significantly greater specificity and affinity to MDM2 when compared to p53 binding, Nutlin-3a binding, and previous analog MI-219 binding (30). Importantly, MI-773 was able to activate p53 activity and induce apoptosis in cancer cells at a much greater efficiency when compared to the standard, nutlin-3a (30). Notably, this therapeutic effect was seen in cell lines with both wild type and mutated p53 (31), as long as they retain an additional wild type copy of the p53 gene.

While the therapeutic effect of MI-773 in inducing tumor cell apoptosis and xenograft tumor regression has been characterized, the effect of MI-773 on cancer stem cells has yet to be determined. The focus of our study is to investigate the therapeutic effect of MI-773 on the cancer stem cells using mucoepidermoid carcinomas as a model of a tumor that follows the cancer stem cell hypothesis (18). Our findings demonstrate that therapeutic inhibition of the MDM2-p53 interaction reduces the fraction of $ALDH^{high}CD44^{high}$ cancer stem cells in mucoepidermoid carcinomas, in addition to inducing apoptosis and cell cycle arrest. Together, these findings unveil inhibitors of MDM2 as a novel strategy for ablation of cancer stem cells.

## Materials and Methods

### Cell culture

A panel of University of Michigan Human Mucoepidermoid Carcinoma cells (UM-HMC-1, UM-HMC-3A, and UM-HMC3B), generated and characterized in our laboratory (32), were cultured using DMEM (Gibco) supplemented with 10% FBS (Gibco), L-Glutamine (Gibco), Penicillin and Streptomycin (Gibco), 20 ng/mL epidermal growth factor (Sigma), 400 ng/mL hydrocortisone (Sigma), 5 μg/mL insulin (Sigma). Primary human microvascular endothelial cells (HDMEC; Lonza) were grown using the EBM2-MV cell culture medium (Lonza).

### Immunohistochemistry and immunofluorescence

Tissue section slides for immunohistochemistry and immunofluorescence staining were deparaffinized using xylene and ethanol, and then incubated with 0.1% Triton-x100 (Sigma) for 10 minutes, 3% hydrogen peroxide for 10 minutes, and Background Sniper (Biocare Medical) for 10–30 minutes. Immunohistochemistry slides were incubated with 1/100 monoclonal anti-human p53 antibody (Santa Cruz, cat #sc-126) or 1/200 monoclonal anti-human MDM2 antibody (Santa Cruz, cat #sc-965) overnight at $4^0$C. Following incubation with primary antibody, sections were washed and then incubated with MACHI 3 Probe

(Biocare Medical) for 20 minutes. After two 10-minute washes, sections were incubated with MACHI 3 HRP polymer for 20 minutes and again washed two times for 10 minutes. Sections were then incubated with DAB for 3 minutes and quenched in water. Sections were finally incubated with hematoxilin for 45 seconds, dehydrated in ethanol and mounted. Immunofluorescence sections were incubated with 1/50 monoclonal anti-human ALDH1 antibody (Abcam, cat #ab52492) overnight at room temperature. The following day, sections were washed and incubated with Alexafluor 488 (Anti-Rabbit; Invitrogen). Then, sections were incubated with 3% hydrogen peroxide for 30 minutes followed by 1-hour incubation with ready to use monoclonal anti-human CD44 antibody (Thermo Scientific, cat #MA5–13890) and a 20-minute incubation with Alexafluor 594 (Anti-Mouse; Invitrogen). Nuclei were stained with DAPI. TUNEL staining was performed using *in situ* TUNEL staining kit (Roche). Seven 200X image fields were taken per tissue section and pixel density was quantitated using ImageJ software.

### Western blots

UM-HMC cells and xenograft MEC tissue lysates were prepared using an NP40-based lysis buffer. Lysates were run using PAGE gels and probed using 1/1000 monoclonal anti-human p53 (Santa Cruz, cat #sc-126), 1/500 monoclonal anti-human MDM2 (Santa Cruz, cat #sc-965), 1/500 monoclonal anti-human p21 (Cell Signaling, cat #2947), 1/1000 monoclonal anti-human Bmi-1 (Cell Signaling, cat #5856), 1/1000 monoclonal anti-human Cyclin-A (Santa Cruz, cat # sc-751), 1/500 monoclonal anti-human Cyclin-D (Santa Cruz, cat # sc-753), 1/1000 monoclonal anti-human Cyclin-E (Cell Signaling, cat #4129), 1/1000 monoclonal anti-human CDK2 (Santa Cruz, cat #sc-6248), 1/500 monoclonal anti-human CDK4 (Santa Cruz, cat # sc-260), 1/1000 monoclonal anti-human CDK6 (Santa Cruz, cat # sc-177), 1/1000 monoclonal anti-human Notch-1 (Cell Signaling, cat #3608s), 1/1000 monoclonal anti-human Notch-2 (Cell Signaling, cat #4530s), 1/1000 monoclonal anti-human Notch-3 (Cell Signaling, cat #5276s), 1/1000 monoclonal anti-human Oct-4 (Cell Signaling, cat #2750s), 1/1000 monoclonal anti-human Nanog (Santa Cruz, cat # sc-293121), and 1/1000 monoclonal anti-human Bcl-$x_L$ (BD Transduction, cat # 610747).

### p53 sequencing

RNA was isolated from sorted and unsorted UM-HMC cells and reverse transcribed. cDNA was PCR-amplified using sense and anti-sense primers targeting full-length p53, as well as residues 54–716, 460–1179, and 876–1412 (33). PCR products were run on a 1.5% agarose gel, fragments were excised and purified for Sanger sequencing performed by the University of Michigan Sequencing Core. In addition, we isolated genomic DNA using the Wizard genomic DNA purification kit (Promega; Madison, WI, USA) and performed Sanger sequencing to evaluate the status of p53 in the UM-HMC cell lines.

### P53 gene silencing

HEK293T cells were transiently co-transfected with the lentiviral packaging vectors psPAX2, pMD2G, and shRNA-p53 (seq#1: TACACATGTAGTTGTAGTG, seq#2: TAACTGCAAGAACATTTCT) or scramble sequence control (shRNA-C) (Vector Core, University of Michigan) by the calcium phosphate method. UM-HMC-3A cells were infected with supernatants containing lentivirus and selected with 1 μg/ml of puromycin

(Sigma-Aldrich, St. Louis, MO) for at least 1 week. Knockdown of p53 was verified by western blot.

### WST-1

UM-HMC cells were plated at a density of 500 cells/well in a 96-well plate and allowed to attached overnight. MI-773 was solubilized in DMSO and added at increasing concentrations (0.01–100 μM) for 24–72 hours (100 μM DMSO served as vehicle control). WST-1 reagent (Roche) was added to cells and incubated at $37^0$C for 4 hours, and plates were analyzed in a microplate reader (GENious; Tecan).

### Flow Cytometry

UM-HMC cells were exposed to 1 μM MI-773, or 1 μM DMSO (vehicle control), for 48–96 hours. For ALDH/CD44 staining, single cell suspensions of 2 million cells/tube were incubated in ALDH substrate (Cayman Chemicals, Ann Arbor, MI), or ALDH inhibitor diethylaminobenzaldehyde (DEAB; Cayman Chemicals), for 40 minutes at $37^0$C, as we described (16). Then, cells were washed and exposed to 1:20 anti-CD44 (APC; BD Pharmingen) for 30 minutes at 4ºC. At least 10,000 events were analyzed per cell type and experimental condition at the University of Michigan Flow Cytometry Core. Results were analyzed using FlowJo® software (FlowJo, LLC). For propidium iodine staining, cells were fixed in 70% ethanol overnight at $-20^0$C and stained in 1 mg/ml propidium iodide (BD Biosciences), 1% sodium citrate (Fisher), 1 mg/ml RNase A (Sigma), 10% Triton X-100 (Fisher) for 20 minutes. For Annexin V staining, cells were washed in PBS then suspended in 1X Binding Buffer (BD Biosciences). Annexin V (APC; BD Biosciences) was added to 100,000 cells and incubated for 20 minutes at room temperature. In all flow cytometry experiments, 7AAD (BD Biosciences) was used as a live/dead control. Data were obtained from triplicate wells and represent at least 3 independent experiments.

### Apoptosis Antibody Array

The Human Apoptosis Array (Catalog #ARY009; R&D Systems) was used to assess the expression of apoptosis associated proteins in vehicle versus MI-773 treated cells. 200,000 UM-HMC-3A cells were seated and treated with 5 μM MI-773 or 5 μM DMSO (vehicle control) for 24 hours. Following treatment, the cells were lysed and analyzed according the company protocol. Array blots were quantitated using ImageJ software.

### Mucoepidermoid carcinoma xenograft tumors

Highly porous poly-L-lactic acid scaffolds were seeded with 600,000 UM-HMC-3A or UM-HMC-3B cells together with 400,000 primary human HDMEC cells (Lonza) in a 1:1 mix of growth factor-reduced (Matrigel; Corning) and EGM2-MV (Lonza), as we described (18,32,34). Scaffolds were implanted in the subcutaneous space of the dorsal region of CB-17 SCID mice (Charles River). Scaffolds were measured weekly until tumors reached an average volume of 500 $mm^3$. Mice were treated daily with 50–200 mg/kg MI-773 or vehicle (polyethylene glycol-200 and D-α-tocopherol polyethylene glycol 100 succinate; Sigma-Aldrich) via oral gavage. After 7 days, mice were euthanized, tumors were removed, and the tissues were digested using the Tumor Dissociation Kit (Miltenyi Biotec, 130-095-929) and

the GentleMACS Dissociator (Miltenyi Biotec) following manufacturer's instructions. Single cell tumor tissue suspensions were stained for flow cytometry, as described above.

## Results

### MDM2 and p53 expression in human mucoepidermoid carcinoma

To investigate the patterns of expression of MDM2 and p53 in human mucoepidermoid carcinoma, we performed Immunohistochemical analyses that revealed strong MDM2 and relatively weaker p53 expression (Fig. 1A). To validate these results in vitro, we performed PCR and Western blot analyses on a panel of human MEC cell lines (UM-HMC) generated and characterized in our laboratory (32), as follows: UM-HMC-1, primary MEC from a minor salivary gland of buccal mucosa; UM-HMC-3A, local MEC recurrence, left hard palate; and UM-HMC-3B, originated from the lymph node metastases of the same patient who donated tissues for UM-HMC-3A. We observed lower p53 mRNA expression in the UM-HMC-3A cells, as compared to UM-HMC-1 and UM-HMC-3B (Fig. 1B). At the protein level, both UM-HMC-1 and UM-HMC-3A cell lines showed strong MDM2 expression and low p53 expression (Fig. 1C). Interestingly, we noticed the opposite pattern in the metastatic UM-HMC-3B cells that showed minimal baseline MDM2 expression and elevated p53 expression (Fig. 1C). We next compared MDM2 and p53 expression in cancer stem cells ($ALDH^{high}CD44^{high}$) and non-cancer stem cells, *i.e.* the pool of remaining cells (control cells). Higher expression of MDM2 was observed in $ALDH^{high}CD44^{high}$ cells when compared to control cells, particularly in cells sorted from sorted from the UM-HMC-3B cell line (Fig. 1D). Expression of p53 remained consistent between $ALDH^{high}CD44^{high}$ and non-cancer stem cells in both cell lines, but p53 was generally stronger in UM-HMC-3B than in UM-HMC-3A (Fig. 1D). Sanger sequencing suggested the presence of A278P polymorphism in UM-HMC-1, UM-HMC-3A, and UM-HMC-3B cells as well as V157F in UM-HMC-3A and UM-HMC-3B cells with retention of wild type alleles. Next, we performed exome sequencing to confirm the presence/absence of mutations that would affect the function of p53 in the UM-HMC cell lines. This analysis revealed that all UM-HMC cell lines studied here have wild-type, functional, *TP53* gene.

### Inhibition of MDM2-p53 interaction with MI-773 reduces the fraction of $ALDH^{high}CD44^{high}$ cells

To evaluate the effect of MI-773 on the fraction of MEC cancer stem cells, we treated UM-HMC-1 cells with 1 μM MI-773 for 48–96 hours and performed FACS analysis for $ALDH^{high}CD44^{high}$ cells. We observed a significant and consistent decrease in the $ALDH^{high}CD44^{high}$ cell population at each time period evaluated (Fig. 2A). To determine whether this decrease was due to selective death (or decrease in proliferation) of the CSC population or differentiation into a non-CSC cell type, we performed a WST-1 analysis. After 72-hour treatment with increasing concentrations of MI-773, we observed no difference in the cytotoxicity curves for $ALDH^{high}CD44^{high}$ cells when compared to control non-CSC cells, suggesting that MI-773-mediated decrease in cancer stem cells (Fig. 2A) is not mediated by preferential killing these cells (Fig. 2B). To verify specificity of these results, we repeated this analysis in UM-HMC-3A and UM-HMC-3B cells and observed a significant decrease in the fraction of $ALDH^{high}CD44^{high}$ cells upon treatment with MI-773

(Fig. 2C,E). As described for UM-HMC-1 above, we did not observe significant differences in the overall cell density of cancer stem cells and control non-CSC cells (Fig. 2D,F). Interestingly, UM-HMC-3B cells were more resistant to MI-773, with $IC_{50s}$ about 10-fold higher than the other 2 MEC cell lines examined here. Together, these results demonstrate that MI-773 reduces the fraction of $ALDH^{high}CD44^{high}$ cells in mucoepidermoid carcinoma cells *in vitro*, and that this effect on cancer stem cells does not correlate with the overall sensitivity of bulk cells to the drug.

To assess the impact of "off-target" effects, we used shRNA vectors to knockdown p53 expression in mucoepidermoid carcinoma cells and exposed the cells to MI-773 (Fig. 3A). While shRNA-p53 sequence #1 was effective in reducing p53 expression, shRNA-p53 sequence #2 showed little effect and was used as an additional control (Fig. 3B). Interestingly, we observed a significant reduction in MDM2 and p21 expression in p53-silenced cells (Fig. 3B), suggesting that indeed these two proteins are downstream targets of p53. We observed that the $IC_{50}$ for MI-773 in p53-silenced cells is approximately 15-fold higher than in vector control cells (Fig. 3A). These results show that p53 silencing enhances resistance of UM-HMC-3A cells to MI-773 treatment and suggests that the therapeutic effect of MI-773 is primarily through the activation of functional p53, and not simply off-target effects.

To determine the overall effect of MI-773 on mucoepidermoid carcinoma cell density and expression of proteins downstream of p53, we performed WST-1 and western blot analyses on unsorted UM-HMC-1, UM-HMC-3A, and UM-HMC-3B cells treated with MI-773. We observed a consistent and dose dependent decrease in total cell number in all MEC cell lines used here (Fig. 3C,E,G). However, it became clear again that the UM-HMC-3B were more resistant to MI-773, with an $IC_{50}$ at 72-hour treatment that was approximately 72-fold higher than the $IC_{50}$ of UM-HMC-1 cells, and about 10-fold higher than the $IC_{50}$ of UM-HMC-3A cells. We performed analysis of covariance on the normalized WST-1% to determine if cell density differences were based on treatment time controlling for concentration of MI-773 using the R 3.1.0 software (35). For cell lines UM-HMC-1, UM-HMC-3A, and UM-HMC-3B, the MI-773 treatment time was significant, controlling for log-concentration ($p < 10^{-6}$; $p < 10^{-6}$; $p = 0.0114$ respectively). We next treated the cells with 0–20 μM MI-773 and observed a robust dose-dependent increase in MDM2, p53, and p21 expression suggesting that p53 signaling is indeed activated in UM-HMC-1 and UM-HMC-3A cells (Fig. 3D,F). In contrast, expression of MDM2, p53, and p21 was not significantly affected by treatment with MI-773 in UM-HMC-3B cells (Fig. 3H). This may begin to explain the resistance that these cells exhibit against inhibition of the MDM2-p53 interaction with MI-773. Surprisingly, we observed a significant reduction of the key regulator of stem cell self-renewal Bmi-1 in the 3 MEC cell lines evaluated here (Fig. 3D,F,H). This observation provides a putative mechanism to explain the reduction in cancer stem cell fraction upon treatment with MI-773 in all cell lines (Fig. 2A,C,E).

### Induction of cell cycle arrest and apoptosis in HMC cells by MI-773

To further investigate the mechanisms underlying MI-773-mediated effects on MEC cell density, we treated UM-HMC cells with low dose MI-773 (1 μM), stained with a hypotonic

solution of propidium iodide and performed flow cytometry. We observed a $G_1$ cell cycle and a correspondent decrease in the fraction of UM-HMC-3A cells in both S and $G_2$/M suggesting that MI-773 did indeed induce $G_1$ cell cycle arrest (Fig. 4A). We repeated this experiment with UM-HMC-1 cells and observed a significant decrease in the fraction of UM-HMC-1 cells in S and $G_2$/M (Supplementary Fig. 1). Indeed, we consistently observed similar trends in cell cycle experiments performed with UM-HMC-1 and UM-HMC-3A. We next treated UM-HMC-3A cells with increasing concentrations of MI-773 to evaluate the effect of MI-773 on apoptosis via staining with both 7AAD and Annexin-V. We observed an increase of cells positive for Annexin-V alone (early apoptosis) as well as cells positive for both Annexin-V and 7AAD (late apoptosis) suggesting that MI-773 induces apoptosis of UM-HMC-3A cells (Fig. 4B). Then, we repeated these experiments with the resistant, UM-HMC-3B cells. MI-773 did not cause changes in the cell cycle distribution of UM-HMC-3B cells (Fig. 4C), and did not induce apoptosis (Fig. 4D). To confirm that indeed MI-773 was mediating UM-HMC-3A cell apoptosis (and not non-specific cell death), we treated UM-HMC-3A cells with MI-773 for 24 hours and ran an Apoptosis Antibody Array (R&D Systems). We observed a significant upregulation (*i.e.* more than 2-fold) of several known inducers of apoptosis, such as Bax, cleaved caspase-3, cytochrome c, and cIAPs (Fig. 4E,F). This assay also confirmed the increase in expression of p53 and p21 (Fig. 4E,F) that was observed in the Western blots (Fig. 3). To evaluate the responses with our resistant cell line (i.e. UM-HMC-3B), we treated these cells with MI-773 and ran an Apoptosis Antibody Array (R&D Systems). As expected, we observed very minor changes (*i.e.* less than 2-fold) in expression of the apoptosis-inducing proteins in UM-HMC-3B cells exposed to MI-773 (Fig. 4G,H). Collectively, these results demonstrate that treatment with MI-773 induces cell cycle arrest and apoptosis in UM-HMC-3A, but not in the resistant UM-HMC-3B cells.

### Effect of therapeutic inhibition of MDM2-p53 interaction on tumor cell apoptosis *in vivo*

To determine the effect of therapeutic inhibition of the MDM2-p53 interaction with MI-773 on tumor cell apoptosis and fraction of cancer stem cells *in vivo*, we transplanted mucoepidermoid carcinoma cells (UM-HMC-3A or UM-HMC-3B) with human microvascular endothelial cells (HDMEC) on a biodegradable scaffold in mice, as previously described (18,34). Once tumors reached an average volume of 500 $mm^3$, mice were treated daily with 100 mg/kg MI-773 by oral gavage. Treatment was performed for a week only, as these experiments were focused on the effects of MI-773 in tumor cell apoptosis and fraction of cancer stem cells (not its effects on tumor size). We observed modest and not statistically significant ($p>0.05$) tumor regression in xenografts generated with UM-HMC-3A cells (Fig. 5A) and in the UM-HMC-3B tumors (Fig. 5B) in mice treated with MI-773. To determine the systemic cytotoxicity of MI-773, we monitored mouse weight during treatment and observed that mice in the treatment group had modest weight loss (Fig. 5C,D).

As an initial readout for MI-773 activity *in vivo*, we examined the effect of this small molecule inhibitor on the expression of MDM2 and p53. Immunohistochemistry revealed a qualitative increase in expression of MDM2 and p53 upon treatment with MI-773 (Fig. 5E). In attempt to quantify these differences, we performed Western blots from tumor tissues retrieved from mice that received MI-773 or vehicle. We observed a substantial increase in

the expression of MDM2, p53 and p21 in UM-HMC-3A tumors treated with MI-773. In contrast, UM-HMC-3B tumor showed modest upregulation of MDM2 and p53, while no changes in p21 expression were observed (Fig. 5F).

Tissue sections were stained for *in situ* TUNEL to determine the effect of MI-773 on apoptosis *in vivo*. Seven standard images were taken from each tumor (N=3 tumors per experimental condition) and pixel density of apoptotic cells was quantitated using ImageJ software. We observed a significant increase in TUNEL-positive cells in the MI-773-treated UM-HMC-3A tumors, when compared to the vehicle treated tumors (Fig. 5G). In contrast, MI-773 did not mediate a significant increase in the number of apoptotic cells in the UM-HMC-3B tumors treated with MI-773 (Fig. 5H).

To determine whether a higher dose of MI-773 would be more effective in UM-HMC-3B tumors, we repeated these experiments treating 5 mice (10 tumors) with a higher dose of MI-773 (*i.e.* 200 mg/kg) as well as 5 mice (10 tumors) with a vehicle control. Again, we did not observe a significant reduction in tumor volume (Supplementary Fig. 2A). But, in this case, we had to discontinue treatment after 5 days as average mouse weight dropped to about 80% of pre-treatment average (Supplementary Fig. 2B). As before, we observed visible upregulation of p53 expression, that was accompanied by decreased expression of $G_1$ cell cycle associated proteins Cyclin A, Cyclin D1, Cyclin E, CDK2, CDK4, and CDK6 in the MI-773 treated tumors when compared to the vehicle treated tumors (Supplementary Fig. 2C,D). We have also confirmed that MI-773 decreases the presence of $ALDH^{high}CD44^{high}$ cells, but does not increase the number of apoptotic cells in UM-HMC-3B tumors (Supplementary Fig. 2E,F).

### Therapeutic inhibition of MDM2-p53 interaction decreases the fraction of cancer stem cells *in vivo*

To define the effect of MI-773 on the fraction of cancer stem cells (*i.e.* $ALDH^{high}CD44^{high}$ cells), we performed immunofluorescence studies using the combination ALDH and CD44 as markers of cancer stem cells in mucoepidermoid carcinoma, as we showed (18). We observed that MI-773 caused a significant decrease in the fraction of cancer stem cells in both, UM-HMC-3A and UM-HMC-3B tumors (Fig. 6A). These data were confirmed by flow cytometry for ALDH activity and CD44 expression from cells retrieved from UM-HMC-3A and UM-HMC-3B tumors treated with MI-773 or vehicle control (Fig. 6B). This is consistent with the *in vitro* data that also showed significant reductions in the cancer stem cell fraction upon treatment with MI-773 (Fig. 2). Interestingly, UM-HMC-3B tumors appear to have a higher baseline fraction of $ALDH^{high}CD44^{high}$ cells as compared to UM-HMC-3A tumors (Fig. 6A,B). In attempt to understand a possible mechanism that explains the decrease in cancer stem cells mediated by MI-773, we performed western blots in both UM-HMC-3A and UM-HMC-3B treated tumor tissue lysates that revealed that MI-773 mediates a substantial reduction in expression levels of the key regulator of self-renewal Bmi-1 (Fig. 6C,D). And finally, we observed that MI-773 mediated dose-dependent inhibition of some stem cell transcription factors (*i.e.* Notch-1, Notch-2), but not Nanog or Oct-4, in mucoepidermoid carcinoma cells, (Fig. 6E). Collectively, these data demonstrate that therapeutic inhibition of MDM2 mediates a decrease in the fraction of

ALDH$^{high}$CD44$^{high}$ cells *in vivo* that is correlated with a decrease in the expression of Bmi-1, a key regulator of stem cell self-renewal.

## Discussion

Resistance to chemotherapy and radiation treatments poses a major challenge to effectively treating patients with advanced stage mucoepidermoid carcinomas. Previous research indicates that cancer stem cells play a critical role in resistance to therapy and disease recurrence (12, 36–37). Studies from our laboratory identified cancer stem cells in salivary gland mucoepidermoid carcinoma (18). This aggressive and uniquely tumorigenic subpopulation of cells can be identified as ALDH$^{high}$CD44$^{high}$ cells. Importantly, we found that ALDH$^{high}$CD44$^{high}$ cells are able to self renew and differentiate into non-cancer stem cells. As cancer stem cells are resistant to treatment, novel therapies aiming the ablation of this uniquely tumorigenic population of cancer stem cells are being proposed. Already much research has been done to target stem cell associated pathways aiming to selectively eliminate the cancer stem cell population in other cancer types. Such pathways include Notch, Wnt, Hedgehog, IL-6, Her-2, and PI3K/AKT (38–41). For many of these pathways, lack of specific targeted agents poses a barrier to effective elimination of the cancer stem cell population. Here, we present studies that provide the conceptual framework for targeted inhibition of the MDM2-p53 interaction as a strategy to ablate cancer stem cells in mucoepidermoid carcinomas.

The tumor suppressor protein p53 plays a critical role in regulating the cell cycle and senescence as well as inducing apoptosis upon oncogenic stress. Importantly, research also suggests that p53 plays an important role in normal stem cell function by actively initiating or repressing several stem cell associated proteins such as Nanog and Oct-4, making it an intriguing pathway to study in the context of cancer stem cells (42). Studies suggest that in the absence of p53, both normal and tumor cells acquire dedifferentiated phenotypes (22–27). MDM2, the main regulator of p53, functions as a E3 ligase signaling p53 for degradation and can also bind p53 to block the transactivation domain of the protein. Inhibition of MDM2 binding to p53 prevents its degradation and activates p53 to function in the cell. Many groups have sought to develop a small molecule inhibitor to block the MDM2/p53 binding interaction. However, many of these inhibitors lack specificity or clinical translatability to be effective therapeutically (43–47).

One promising inhibitor of the MDM2-p53 interaction, MI-773, is significantly more specific and shows improved anti-tumor efficacy when compared to other small molecule inhibitors (30). Upon treatment with MI-773, researchers observed a significant induction of p53 signaling in a variety of different cancer types (30). Activation of p53 induced apoptosis, which in turn caused significant tumor shrinkage in *in vivo* models (30). Importantly, in our studies MI-773 showed significant therapeutic efficacy against both cancer stem cells and differentiated mucoepidermoid carcinoma cells. Upon treatment with MI-773, we observed a significant reduction of ALDH$^{high}$CD44$^{high}$ cancer stem cells in our mucoepidermoid carcinoma models *in vitro* and *in vivo*. Interestingly, when we treated both ALDH$^{high}$CD44$^{high}$ and non-cancer stem cells with increasing concentrations of MI-773 *in vitro*, we saw no difference (between cancer stem cells and non-cancer stem cells) in the

total cell number. This suggests that the reduction in the fraction of $ALDH^{high}CD44^{high}$ cells is due to induction of their differentiation and/or inhibition of their self-renewal, rather than enhanced susceptibility to apoptosis (in comparison with non-cancer stem cells). To further support this observation, we observed a significant reduction in expression levels of the self-renewal regulator Bmi-1, and an increase in the expression of the differentiation-associated protein p21, in tumors treated with MI-773 *in vivo*.

Using unsorted cells, we observed that MI-773 induces cell cycle arrest and apoptosis in UM-HMC-1 and UM-HMC-3A cells (but not in UM-HMC-3B) *in vivo* and *in vitro*. A possible explanation for this unexpected finding is that the MDM2 expression is lower at baseline in UM-HMC-3B when compared to UM-HMC-1 and UM-HMC-3A cells. As such, these cells might be intrinsically less dependent upon the pro-survival function of MDM2. On the other hand, we observed an increase in TUNEL-positive cells and a decrease in the fraction of cancer stem cells and in the expression of cell cycle-associated proteins in UM-HMC-3B treated with MI-773 *in vivo.* This suggests the tumor microenvironment generated *in vivo* modifies the sensitivity of the UM-HMC-3B cells to MDM2 inhibition. Mechanistic studies are being conducted to test this hypothesis and understand better the reasons for the different behavior of UM-HMC-3B cells *in vitro* and *in vivo*.

While little is known about the role of p53 and MDM2 in salivary gland mucoepidermoid carcinomas, sequencing and immunohistochemistry studies suggest that *TP53* mutations and loss of heterozygosity are rare events in these tumors (48). Interestingly, we observed the *TP53* gene was fully functional in our UM-HMC-1, UM-HMC-3A, and UM-HMC-3B cell lines. This, together with the results presented here, suggests that small molecule inhibitors of the MDM2-p53 interaction might have a place in the therapeutic “armamentarium” considered for treatment of salivary mucoepidermoid carcinomas.

Collectively, this work demonstrates that therapeutic inhibition of the MDM2-p53 binding targets and ablates $ALDH^{high}CD44^{high}$ cancer stem cells in mucoepidermoid carcinomas through activation of p53 and inhibition of stem cell self-renewal *in vitro* and *in vivo*. Activation of p53 by inhibition of MDM2 binding also induces cell cycle arrest and apoptosis in mucoepidermoid carcinoma cells leading to cell death. Notably, a recent Phase I clinical trial (NCT01636479) concluded that MI-773 (*i.e.* SAR405838) was well tolerated in patients with advanced solid tumors (49). These studies suggest that patients with mucoepidermoid carcinoma might benefit from ablation of cancer stem cells using clinically relevant small molecule inhibitors of the MDM2-p53 interaction.

## Supplementary Material

Refer to Web version on PubMed Central for supplementary material.

## Acknowledgements

We thank the patients who kindly provided the tumor specimens used to generate the mucoepidermoid carcinoma cell lines and xenograft models that enabled this research project. We also thank the surgeons, nurses and support staff that enabled the process of tumor specimen collection and processing for use in research as well as the University of Michigan Sequencing and Flow Cytometry Cores for their support.

Financial Support

This work was funded by the University of Michigan Head Neck SPORE P50-CA-97248 from the NIH/NCI; and grants R01-DE21139 and R01-DE23220 from the NIH/NIDCR (JEN) and K08-DE026500 from the NIH/NIDCR (ATP).

## References

1. Spiro RH. Salivary neoplasms: overview of a 35-year experience with 2807 patients. Head Neck Surg 1986;8:177–84. [PubMed: 3744850]
2. Eversole LR, Sabes WR, Rovin S. Aggressive growth and neoplastic potential of odontogenic cysts: with special reference to central epidermoid and mucoepidermoid carcinomas. Cancer 1975;35:270–82. [PubMed: 1089038]
3. Ezsias A, Sugar AW, Milling MA, Ashley KF. Central mucoepidermoid carcinoma in a child. J Oral Maxillofac Surg 1994;52:512–5. [PubMed: 8169719]
4. Ellis GL, Auclair PL. Tumors of the salivary glands - Atlas of tumor pathology. In: Fascicle 17 Washington: Armed Forces Institute of, Pathology; 1996.
5. Gingell JC, Beckerman T, Levy BA, Snider LA. Central mucoepidermoid carcinoma. Review of the literature and report of a case associated with an apical periodontal cyst. Oral Surg Oral Med Oral Pathol 1984;57:436–40. [PubMed: 6584842]
6. Ito FA, Ito K, Vargas PA, de Almeida OP, Lopes MA. Salivary gland tumors in a brazilian population: a retrospective study of 496 cases. Int J Oral Maxillofac Surg 2005;34:533–6. [PubMed: 16053874]
7. Luna MA. Salivary mucoepidermoid carcinoma: revisited. Adv Anat Pathol 2006;13:293–307. [PubMed: 17075295]
8. Pires FR, de Almeida OP, de Araujo VC, Kolawski LP. Prognostic factors in head and neck mucoepidermoid carcinoma. Arch Otolaryngol Head Neck Surg 2004;130:174–80. [PubMed: 14967746]
9. Bell D, Holsinger CF, El-Naggar AK. CRTC1/MAML2 fusion transcript in central mucoepidermoid carcinoma of mandible–diagnostic and histogenetic implications. Ann Diagn Pathol 2010;14:396–401. [PubMed: 21074686]
10. Chen AM, Granchi PJ, Garcia J, Bucci MK, Fu KK, Eisele DW. Local-regional recurrence after surgery without postoperative irradiation for carcinomas of the major salivary glands: implications for adjuvant therapy. Int J Radiat Oncol Biol Phys 2007;67:982–7. [PubMed: 17241753]
11. O'Neill ID. t(11;19) translocation and CRTC1–MAML2 fusion oncogene in mucoepidermoid carcinoma. Oral Oncol 2009;45:2–9. [PubMed: 18486532]
12. Adams A, Warner K, Nör JE. Salivary gland cancer stem cells. Oral Oncol 2013;49:845–53. [PubMed: 23810400]
13. Hambardzumyan D, Squatrito M, Holland EC. Radiation resistance and stem-like cells in brain tumors. Cancer Cell 2006;10:454–6. [PubMed: 17157785]
14. Korkaya H, Paulson A, Charafe-Jauffret E, Ginestier C, Brown M, Dutcher J, et al. Regulation of mammary stem/progenitor cells by PTEN/Akt/beta-catenin signaling. PLoS Biol 2009; 7:e1000121. [PubMed: 19492080]
15. Diehn M, Cho RW, Lobo NA, Kalisky T, Dorie MJ, Kulp AN, et al. Association of reactive oxygen species levels and radioresistance in cancer stem cells. Nature 2009;458:780–3. [PubMed: 19194462]
16. Ailles LE, Weissman IL. Cancer stem cells in solid tumors. Curr Opin Biotechnol 2007;18:460–6. [PubMed: 18023337]
17. Diehn M, Cho RW, Clarke MF. Therapeutic implications of the cancer stem cell hypothesis. Semin Radiat Oncol 2009;19:78–86. [PubMed: 19249645]
18. Adams A, Warner K, Pearson AT, Zhang Z, Kim HS, Mochizuki D, et al. ALDH/CD44 identifies uniquely tumorigenic cancer stem cells in salivary gland mucoepidermoid carcinomas. Oncotarget 2015;6:26633–50. [PubMed: 26449187]

19. Fridman JS, Lowe SW. Control of apoptosis by p53. Oncogene 2003;22:9030–40. [PubMed: 14663481]
20. Vogelstein B, Lane D, Levine AJ. Surfing the p53 network. Nature 2000;408:307–10. [PubMed: 11099028]
21. Vousden KH, Lu X. Live or let die: the cell's response to p53. Nat Rev Cancer 2000;2:594–604.
22. Marión RM, Strati K, Li H, Murga M, Blanco R, Ortega S, et al. A p53-mediated DNA damage response limits reprogramming to ensure iPS cell genomic integrity. Nature 2009;460:1149–53. [PubMed: 19668189]
23. Hong H, Takahashi K, Ichisaka T, Aoi T, Kanagawa O, Nakagawa M et al. Suppression of induced pluripotent stem cell generation by thep53-p21 pathway. Nature 2009;460:1132–5. [PubMed: 19668191]
24. Utikal J, Polo JM, Stadtfeld M, Maherali N, Kulalert W, Walsh RM, et al. Immortalization eliminates a roadblock during cellular reprogramming into iPS cells. Nature 2009;460:1145–8. [PubMed: 19668190]
25. Li H, Collado M, Villasante A, Strati K, Ortega S, Cañamero M, et al. The Ink4/Arf locus is a barrier for iPS cell reprogramming. Nature 2009;460:1136–9. [PubMed: 19668188]
26. Kawamura T, Suzuki J, Wang YV, Menendez S, Morera LB, Raya A, et al. Linking the p53 tumour suppressor pathway to somatic cell reprogramming. Nature 2009;460:1140–4. [PubMed: 19668186]
27. Tschaharganeh DF, Xue W, Calvisi DF, Evert M, Michurina TV, Dow LE, et al. p53-dependent Nestin regulation links tumor suppression to cellular plasticity in liver cancer. Cell 2014;158:579–92. [PubMed: 25083869]
28. Momand J, Zambetti GP, Olson DC, George D, Levine AJ. The mdm-2 oncogene product forms a complex with the p53 protein and inhibits p53-mediated transactivation. Cell 1992;69:1237–45. [PubMed: 1535557]
29. Mantesso A, Loducca SV, Bendit I, Garicochea B, Nunes FD, de Araújo VC. MDM2 mRNA expression in salivary gland tumour cell lines. J Oral Pathol Med 2004;33:96–101. [PubMed: 14720195]
30. Wang S, Sun W, Zhao Y, McEachern D, Meaux I, Barrière C, et al. SAR405838: an optimized inhibitor of MDM2-p53 interaction that induces complete and durable tumor regression. Cancer Res 2014;74:5855–65. [PubMed: 25145672]
31. Hoffman-Luca CG, Yang CY, Lu J, Ziazadeh D, McEachern D, Debussche L, et al. Significant Differences in the Development of Acquired Resistance to the MDM2 Inhibitor SAR405838 between In Vitro and In Vivo Drug Treatment. PLoS One 2015;10:e0128807. [PubMed: 26070072]
32. Warner KA, Adams A, Bernardi L, Nor C, Finkel KA, Zhang Z, et al. Characterization of tumorigenic cell lines from the recurrence and lymph node metastasis of a human salivary mucoepidermoid carcinoma. Oral Oncol 2013;49:1059–66. [PubMed: 24035723]
33. Bauer JA, Trask DK, Kumar B, Los G, Castro J, Lee JS, Chen J, Wang S, Bradford CR, Carey TE. Reversal of cisplatin resistance with a BH3 mimetic, (−)-gossypol, in head and neck cancer cells: role of wild-type p53 and Bcl-xL. Mol Cancer Ther 2005;4:1096–104. [PubMed: 16020667]
34. Nör JE, Peters MC, Christensen JB, Sutorik MM, Linn S, Khan MK, Addison CL, Mooney DJ, Polverini PJ. Engineering and characterization of functional human microvessels in immunodef cient mice. Lab Invest 2001; 81: 453–463. [PubMed: 11304564]
35. R Development Core Team (2008). R: A language and environment for statistical computing R Foundation for Statistical Computing, Vienna, Austria ISBN 3-900051-07-0, URL http://www.R-project.org
36. Hambardzumyan D, Squatrito M, Holland EC. Radiation resistance and stem-like cells in brain tumors. Cancer Cell 2006;10:454–6. [PubMed: 17157785]
37. Shafee N, Smith CR, Wei S, Kim Y, Mills GB, Hortobagyi, et al. Cancer stem cells contribute to cisplatin resistance in Brca1/p53-mediated mouse mammary tumors. Cancer Res 2008;68:3243–50. [PubMed: 18451150]
38. Takabe N, Harris PJ, Warren RQ, Ivy SP. Targeting cancer stem cells by inhibiting Wnt, Notch, and Hedgehog pathways. Nat Rev Clin Oncol 2011;8:97–106. [PubMed: 21151206]

39. Krishnamurthy S, Warner KA, Dong Z, Imai A, Nör C, Ward BB, et al. Endothelial interleukin-6 de nes the tumorigenic potential of primary human cancer stem cells. Stem Cells 2014;32:2845–57. [PubMed: 25078284]
40. Li X, Lewis MT, Huang J, Gutierrez C, Osborne CK, Wu MF, et al. Intrinsic resistance of tumorigenic breast cancer cells to chemotherapy. J Natl Cancer Inst 2008;100:672–9. [PubMed: 18445819]
41. Kolev VN, Wright QG, Vidal CM, Ring JE, Shapiro IM, Ricono J, et al. PI3K/mTOR dual inhibitor VS-5584 preferentially targets cancer stem cells. Cancer Res 2015 ;75:446–55. [PubMed: 25432176]
42. Kawamura T, Suzuki J, Wang YV, Menendez S, Morera LB, Raya A, et al. Linking the p53 tumour suppressor pathway to somatic cell reprogramming. Nature 2009;460:1140–4. [PubMed: 19668186]
43. Vassilev LT, Vu BT, Graves B, Carvajal D, Podlaski F, Filipovic Z, et al. In vivo activation of the p53 pathway by small-molecule antagonists of MDM2. Science 2004;303:844–8. [PubMed: 14704432]
44. Shangary S, Qin D, McEachern D, Liu M, Miller RS, Qiu S, et al. Temporal activation of p53 by a specific MDM2 inhibitor is selectively
toxic to tumors and leads to complete tumor growth inhibition. Proc Natl Acad Sci U S A 2008;105:3933–8. [PubMed: 18316739]
45. Vassilev LT. p53 Activation by small molecules: application in oncology. J Med Chem 2005;48:4491–9. [PubMed: 15999986]
46. Vassilev LT. MDM2 inhibitors for cancer therapy. Trends Mol Med 2007;13:23–31. [PubMed: 17126603]
47. Carry JC, Garcia-Echeverria C. Inhibitors of the p53/hdm2 protein-protein interaction-Path to the clinic. Bioorg Med Chem Letters 2013; 23:2480–5.
48. Gomes CC, Diniz MG, Orsine LA, Duarte AP, Fonseca-Silva T, Conn BI, et al. Assessment of TP53 mutations in benign and malignant salivary gland neoplasms. PLoS One 2012;7:e41261. [PubMed: 22829934]
49. de Jonge M, de Weger VA, Dickson MA, Langenberg M, Le Cesne A, Wagner AJ, et al. A phase I study of SAR405838, a novel human double minute 2 (HDM2) antagonist, in patients with solid tumours. Eur J Cancer 2017;76:144–151 [PubMed: 28324749]

## Translational relevance

Mucoepidermoid carcinoma is the most common tumor of the salivary gland. The development of targeted therapies has been hindered by the scarcity of experimental models and by poor understanding of the pathobiology of this cancer. As such, treatment is frequently limited to surgery and radiation. Using a panel of mucoepidermoid carcinoma cell lines generated in our laboratory, we have recently reported that this tumor relies on the function of cancer stem cells endowed with multipotency, capacity of self-renew and unique tumorigenic potential. Here, we present a novel strategy for ablation of these cancer stem cells that is based on the therapeutic blockade of the MDM2-p53 interaction. We showed that single agent MI-773 (small molecule inhibitor of MDM2-p53) is sufficient to ablate the highly tumorigenic cancer stem cells in preclinical models of mucoepidermoid carcinoma. These results suggest that patients with mucoepidermoid carcinoma might benefit from therapeutic inhibition of the MDM2-p53 interaction.

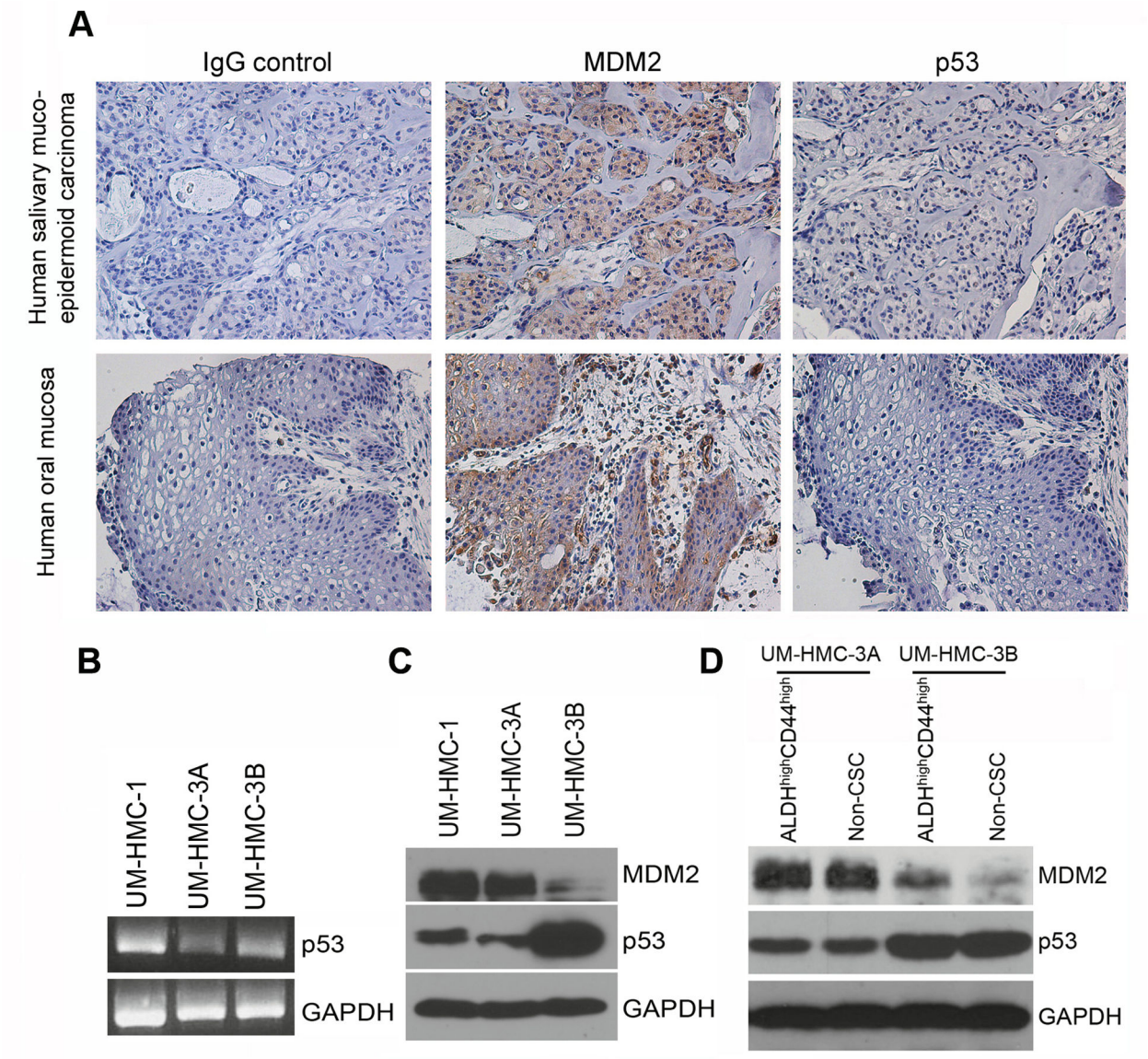


**Figure 1.**

MDM2 and p53 expression in human salivary gland mucoepidermoid carcinoma and HMC cell lines. A, Representative images of immunohistochemistry staining for MDM2 and p53 in one patient with salivary gland mucoepidermoid carcinoma and control oral mucosa. Images were taken at 200X. B, PCR analysis of total p53 RNA levels in UM-HMC-1, UM-HMC-3A, and UM-HMC-3B cells. C, Western blot analysis of p53 and MDM2 expression in UM-HMC-1, UM-HMC-3A, and UM-HMC-3B cells. D, Western blot analysis of p53 and MDM2 expression in UM-HMC-3A and UM-HMC-3B cells FACS sorted for both the $ALDH^{high}CD44^{high}$ cancer stem cell population and the remaining cells that were not $ALDH^{high}CD44^{high}$ (*i.e.* non-cancer stem cells).

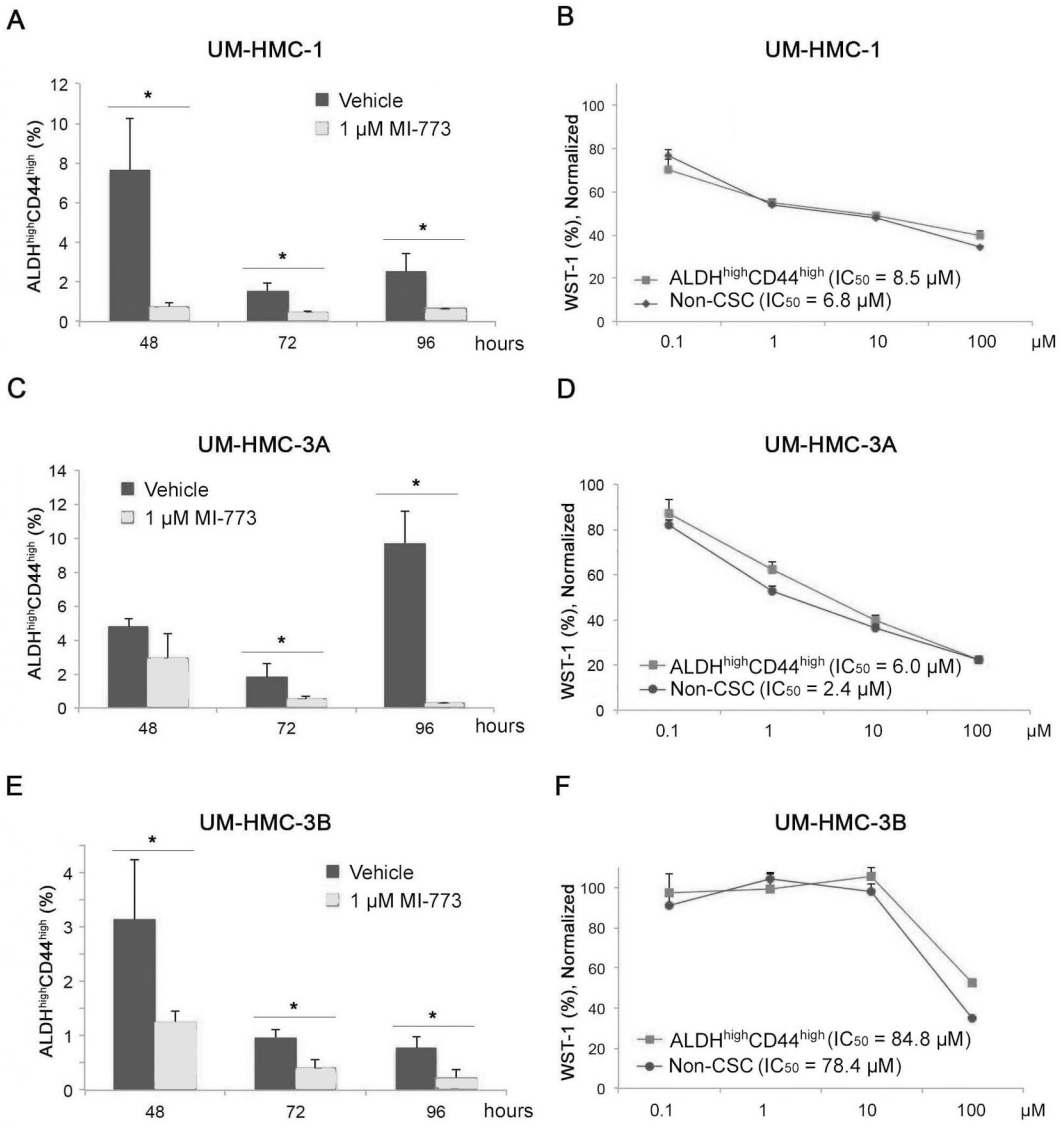


**Figure 2.**

Effect of MDM2/p53 binding inhibition by MI-773 on the ALDH$^{high}$CD44$^{high}$ population in HMC cells. A, FACS analysis of UM-HMC-1 cells after 48, 72, and 96-hour treatments with 1uM MI-773. Cells were plated at 500,000 cells per flask and treated with 1uM MI-773. After the 48, 72, and 96-hour time points, the cells were detached and analyzed for the ALDH$^{high}$CD44$^{high}$ cancer stem cells population. B, WST-1 analysis of UM-HMC-1 cells FACS sorted for the ALDH$^{high}$CD44$^{high}$ cancer stem cells and the non-ALDH$^{high}$CD44$^{high}$ cells population. After sorting, cells were plated at 500 cells per well in a 96 well tissue culture plate. Once seated, a concentration gradient (0.1 μM-100 μM) of MI-773 was added and cells were exposed for 72 hours. Following the 72 hours treatment, 10uL of WST-1 reagent was added for 4 hours after which the plates were analyzed. C, FACS analysis of UM-HMC-3A cells after 48, 72, and 96-hour treatments with 1uM MI-773. Cells were plated at 500,000 cells per flask and treated with 1uM MI-773. After the 48, 72, and 96-hour

time points, the cells were detached and analyzed for the $ALDH^{high}CD44^{high}$ marker combination. D, WST-1 analysis of UM-HMC-3A cells FACS sorted for the $ALDH^{high}CD44^{high}$ cancer stem cells and the non-$ALDH^{high}CD44^{high}$ cells population. After sorting, cells were plated at 500 cells per well in a 96 well tissue culture plate. Once seated, a concentration gradient (0.1uM-100uM) of MI-773 was added and cells were exposed for 72 hours. Following the 72 hours treatment, 10uL of WST-1 reagent was added for 4 hours and after which the plates were analyzed. E, FACS analysis of UM-HMC-3B cells after 48, 72, and 96-hour treatments with 1uM MI-773. Cells were plated at 500,000 cells per flask and treated with 1uM MI-773. After the 48, 72, and 96-hour time points, the cells were detached and analyzed for the $ALDH^{high}CD44^{high}$ marker combination. F, WST-1 analysis of UM-HMC-3B cells FACS sorted for the $ALDH^{high}CD44^{high}$ cancer stem cells and the non-$ALDH^{high}CD44^{high}$ cells population. After sorting, cells were plated at 500 cells per well in a 96 well tissue culture plate. Once seated, a concentration gradient (0.1uM-100uM) of MI-773 was added and cells were exposed for 72 hours. Following the 72 hours treatment, 10uL of WST-1 reagent was added for 4 hours and after which the plates were analyzed. Bars in this figure indicate the standard deviation.

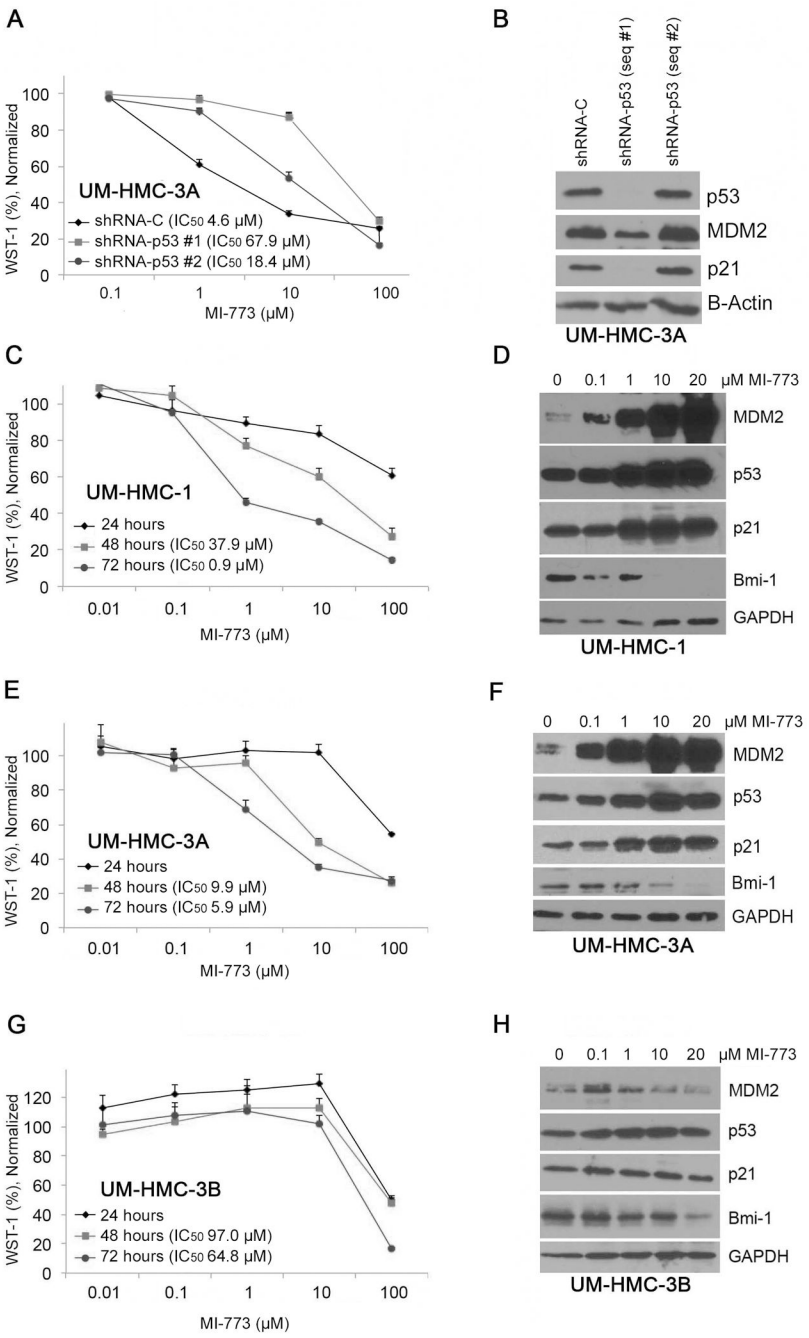


**Figure 3.**

Effect of MDM2/p53 binding inhibition by MI-773 on HMC cell number. A, WST-1 analysis of UM-HMC-3A sh-Control and shp53 cells. p53 was knocked down using three different lentiviral shp53 vectors. Transfected cells were plated at 500 cells per well and exposed to varying concentrations of MI-773 for 72 hours. After 4 hours of incubation with WST-1, the plates were analyzed and normalized to a DMSO control. B, Western blot analysis of lysates created from shp53 knockdown cells. C, WST-1 analysis of UM-HMC-1 cells treated with varying concentrations of MI-773 for 24, 28, and 72 hours. UM-HMC-1

cells were seated at 500 cells per well. After each time point, 10 μL of WST-1 reagent was added to the cells for 4 hours and then analyzed. All cells were normalized to a DMSO control. D, Western blot analysis of UM-HMC-1 cells treated with 0.1, 1, 10, or 20 μM MI-773 for 24 hours. E, WST-1 analysis of UM-HMC-3A cells treated with varying concentrations of MI-773 for 24, 28, and 72 hours. UM-HMC-3A cells were seated at 500 cells per well. After each time point, 10uL of WST-1 reagent was added to the cells for 4 hours and then analyzed. All cells were normalized to a DMSO control. F, Western blot analysis of UM-HMC-3A cells treated with 0.1, 1, 10, or 20 μM MI-773 for 24 hours. G, WST-1 analysis of UM-HMC-3B cells treated with varying concentrations of MI-773 for 24, 28, and 72 hours. UM-HMC-3B cells were seated at 500 cells per well. After each time point, 10uL of WST-1 reagent was added to the cells for 4 hours and then analyzed. All cells were normalized to a DMSO control. H, Western blot analysis of UM-HMC-3B cells treated with 0.1, 1, 10, or 20 μM MI-773 for 24 hours. Bars indicate the standard deviation.

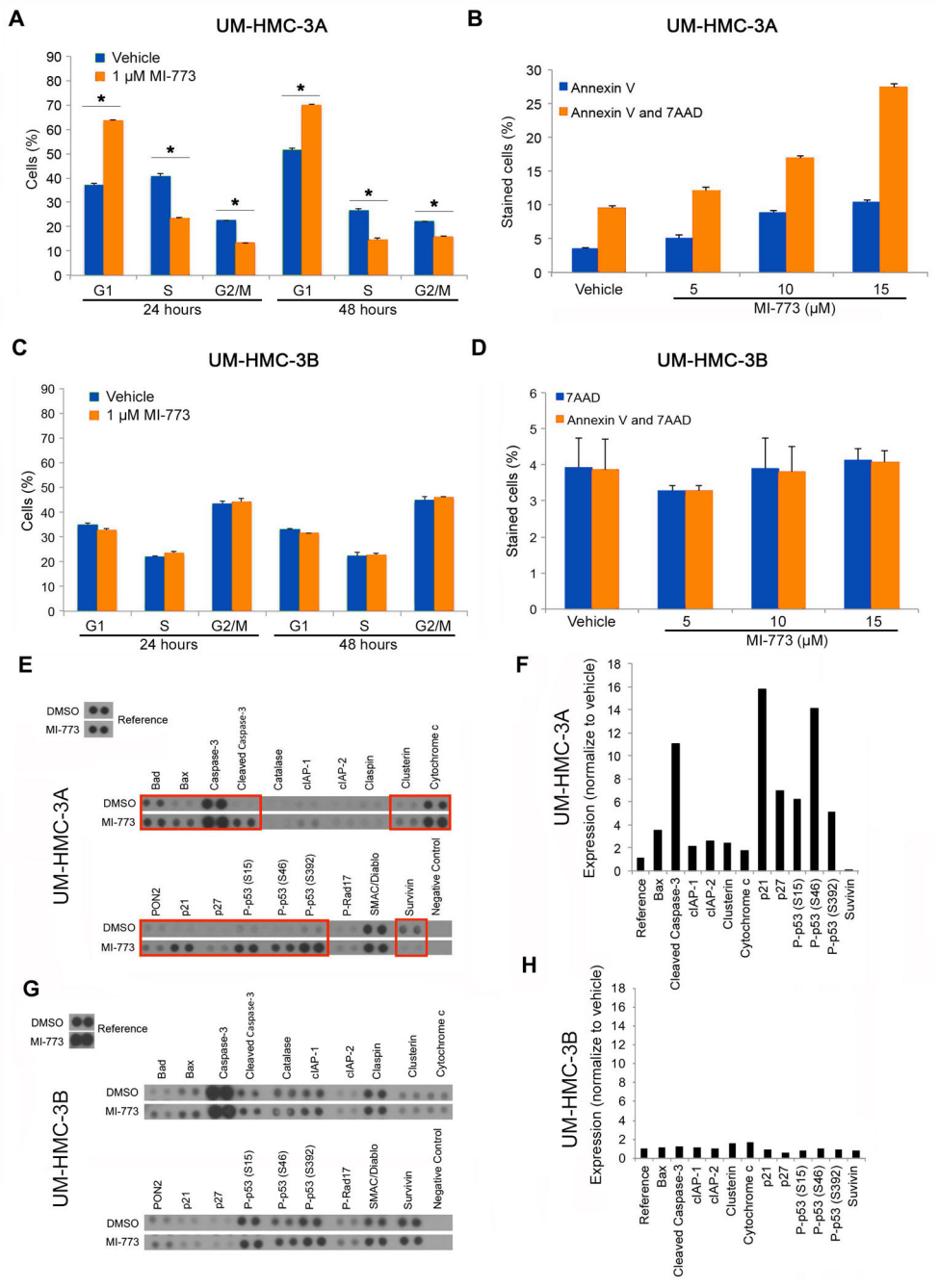


**Figure 4.**

Induction of cell cycle arrest and apoptosis in HMC cells by MI-773. A, Cell cycle analysis of UM-HMC-3A cells treated with 1uM MI-773 for 24 and 48 hours. Cells were plated at 500,000 cells per flask. Control cells were treated with DMSO. B, Annexin V and 7AAD FACS analysis following treatment of UM-HMC-3A cells with 5, 10, or 15 μM MI-773 for 24 hours. Control cells were treated with DMSO. C, Cell cycle analysis of UM-HMC-3B cells treated with 1 μM MI-773 for 24 and 48 hours. Cells were plated at 500,000 cells per flask. Control cells were treated with DMSO. D, Annexin V and 7AAD FACS analysis

following treatment of UM-HMC-3B cells with 5, 10, or 15 μM MI-773 for 24 hours. Control cells were treated with DMSO. E,G, Apoptosis Antibody Array (R&D) analysis in UM-HMC-3A cells (E) or UM-HMC-3B cells (G) treated with 5 μM MI-773 for 24 hours. F,H, Blot from Apoptosis Array performed with in UM-HMC-3A cells (F) or UM-HMC-3B cells (H) was quantitated using ImageJ software. Blot quantitation for MI-773 treated lysates were normalized to the values of the DMSO treated blots. Bars indicate the standard deviation.

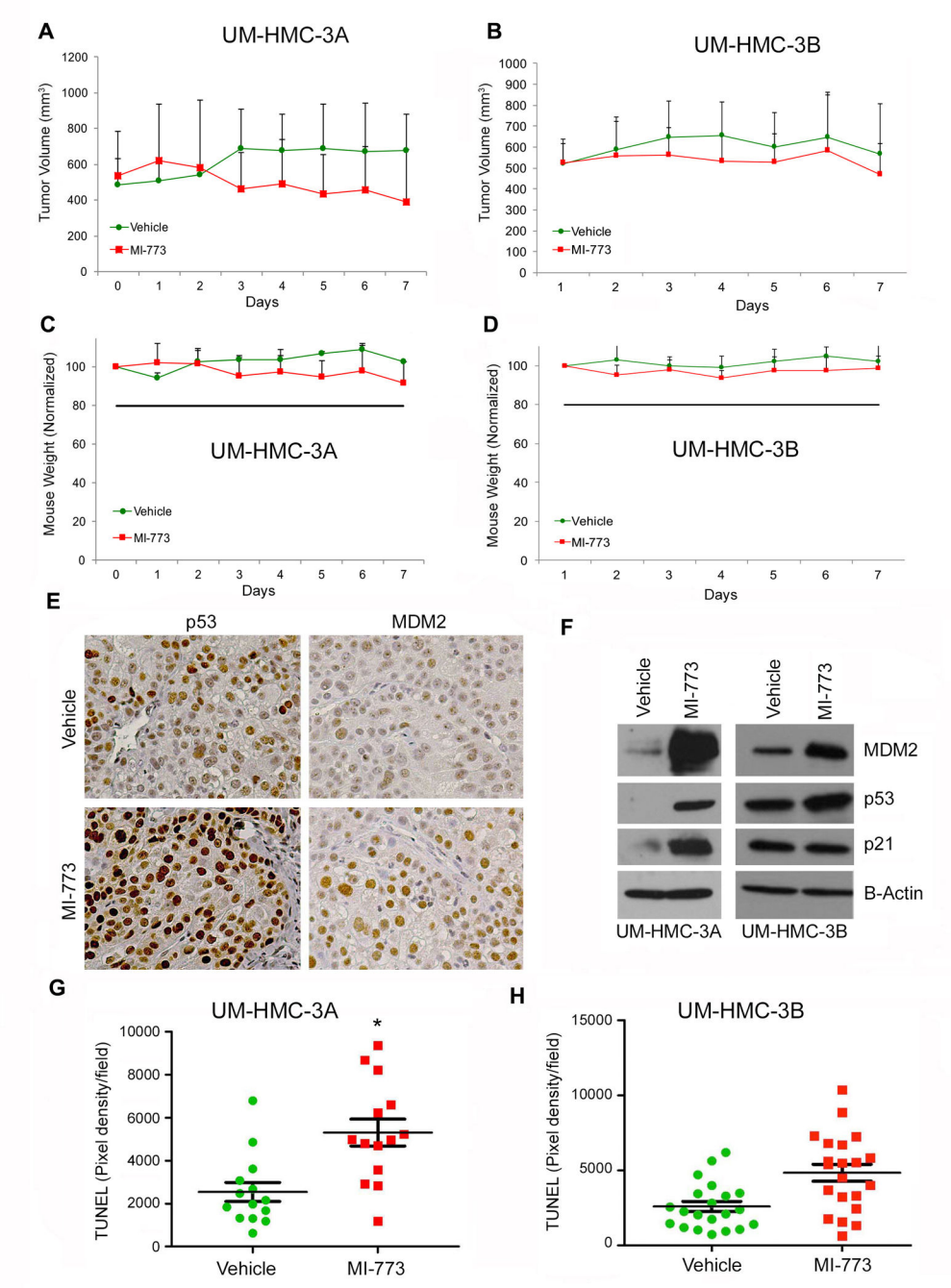


**Figure 5.**

Effect of MDM2/p53 binding inhibition by MI-773 on cancer stem cells in UM-HMC-3A cells *in-vivo*. A, Graph depicting the tumor volume during 6 days of 100 mg/kg treatment with MI-773. 600,000 UM-HMC-3A cells were co-implanted with 400,000 human endothelial cells (HDMEC) on biodegradable scaffolds in the subcutaneous space of SCID mice (N=4 tumors per experimental condition). Once tumor reached an average volume of 500 $mm^3$, the mice were treated by daily oral gavage with 100 mg/kg MI-773 or a vehicle control. B, Graph depicting the tumor volume during 6 days of 100 mg/kg treatment with

MI-773. 600,000 UM-HMC-3B cells were co-implanted with 400,000 human endothelial cells (HDMEC) on biodegradable scaffolds in the subcutaneous space of SCID mice (N=10 tumors per experimental condition). Once tumor reached an average volume of 500 $mm^3$, the mice were treated by daily oral gavage with 100 mg/kg MI-773 or a vehicle control. C, Graph depicting the average mouse weight of UM-HMC-3A implanted mice during the 6-day treatment sequence. D, Graph depicting the average mouse weight in UM-HMC-3B implanted mice during the 6-day treatment sequence. E, Immunohistochemistry analysis of UM-HMC-3A MI-773 or vehicle treated tumors. Images were taken at 200X. F, Western blot analysis of tissue from vehicle and MI-773 UM-HMC-3A and UM-HMC-3B tumors. G,H, Graph depicting the pixel density per field of sections stained for TUNEL in UM-HMC-3A (G) or UM-HMC-3B (H) tumors in mice treated with MI-773 or vehicle control. Seven fields at 200X were taken per tumor section and quantified using the ImageJ software. Error bars indicated the standard error of the mean.

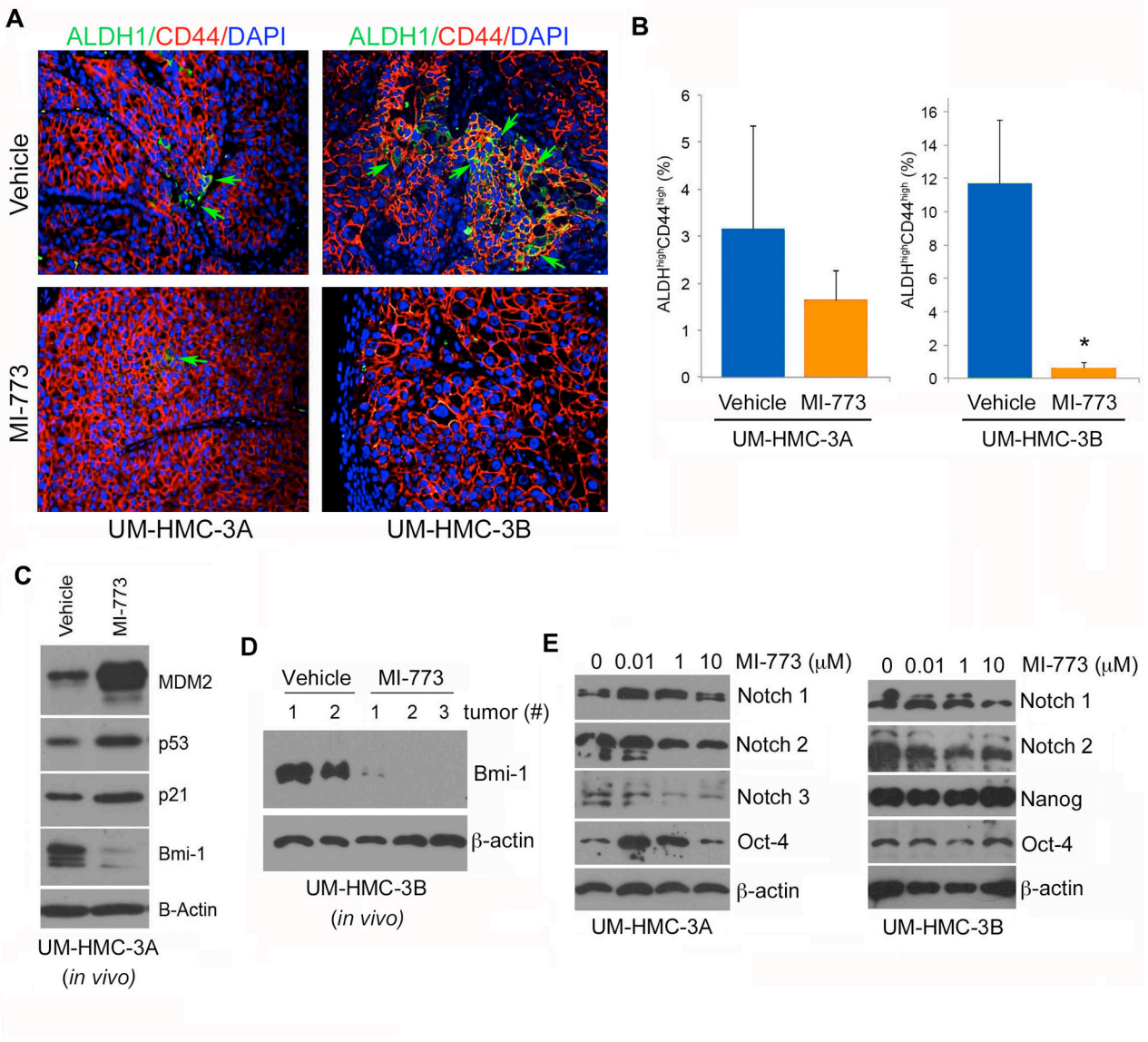


**Figure 6.**

Effect of MDM2/p53 binding inhibition by MI-773 on cancer stem cells in UM-HMC-3B cells *in-vivo*. A, Immunofluorescence analysis of UM-HMC-3A and UM-HMC-3B tumors for ALDH and CD44. Images were taken at 200X. B, Graph depicting the percentage of $ALDH^{high}CD44^{high}$ cells in MI-773 treated UM-HMC-3A and UM-HMC-3B tumors. After 6 days of treatment, the tumors were resected and digested into a single cells suspension. The cells were then stained and FACS analyzed. A t-test was used to test for significance. Error bars indicate the standard deviation. C, Western blot analysis of tissue lysate from UM-HMC-3A vehicle and MI-773 treated tumors. D, Western blot analysis of tissue lysates from xenograft tumor generated with UM-HMC-3B cells that were treated with MI-773 (3 independent tumors) or control (2 independent tumors). E, Western blot analyses of stem cell transcription factors (i.e. Notch-1, Notch-2, Notch-3, Oct-4 and Nanog) in UM-HMC-3A and UM-HMC-3B exposed to 0–10 μM MI-773 for 24 hours.